Materials and Chemistry
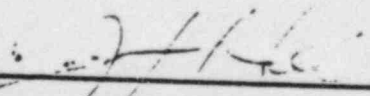
POWER SYSTEMS

COMBUSTION ENGINEERING INC

DESTRUCTIVE EXAMINATION
OF TUBE L29R84 FROM THE
B STEAM GENERATOR AT
FORT CALHOUN

JUNE 1984

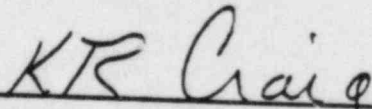D. E. POWELL
J. F. HALL

Reviewed by: _____
J. F. Hall

Approved by: _____
K. R. Craig

COMBUSTION ENGINEERING, INC.
NUCLEAR POWER SYSTEMS
1000 PROSPECT HILL ROAD
WINDSOR, CONNECTICUT 06095

Section 1.0

SUMMARY

Combustion Engineering, Inc. has completed a detailed destructive examination of a failed steam generator tube (L29R84) removed from the Ft. Calhoun Station. Tube failure occurred during plant heat-up following a refueling outage and resulted in a leak exceeding 100 gpm. The analysis indicated that the cause of failure was intergranular stress corrosion cracking which propagated essentially throughwall prior to the final ductile rupture. The examination of the stress corrosion cracks and deposits removed from the tube failed to identify a causative species for the failure. The tube was confirmed to be typical of mill annealed NiCrFe Alloy 600 tubing used in C-E supplied steam generators.

Based on the information available, it was concluded that the failure was most likely the result of caustic stress corrosion cracking with the caustic environment resulting from the concentration in steam blanketed areas of condenser cooling water in-leakage.

1254A0042A

Section 2.0

INTRODUCTION

A large leak (>100 gpm) developed in the B steam generator at Ft. Calhoun Station during plant heat-up following a refueling outage in 1984. Subsequent non-destructive inspection indicated a large throughwall defect in tube L29R84 in the area of the first (hot leg) vertical support strap on the horizontal run. The location of the failure in the horizontal run and the location of the tube in the second peripheral row of tube made removal of the failed section possible. Accordingly, Combustion Engineering removed by cutting with a TIG torch that part of tube L29R84 extending from near the hot-leg 90° bend to the center vertical support. To gain access to tube L29R84, C-E removed an equivalent section of tube L29R86, a first peripheral row tube. After a brief on-site visual examination, the removed sections of both tubes were shipped to C-E's laboratory facilities for detailed non-destructive examinations. The examinations included the following tasks:

1. Laboratory eddy current testing (ECT)
2. Visual examination and documentation of the as-received tube segments
3. Dimensional measurements
4. Light microscoopy examinations
5. Scanning electron microscopy examinations
6. Quantitative and qualitative chemical analyses of tube materials and deposits.

This report documents the results of the laboratory examinations of segments of tube L29R84.

Section 3.0

VISUAL EXAMINATIONS

C-E received two sections, identified as 23B and 23C, from the horizontal run of tube L29R84. Tube section 23B was the length of tube extending from near the hot leg 90° bend to the inboard side of the first vertical tube support, and contained the throughwall defect. Tube section 23C was the section of the same tube extending from inboard of the first vertical support to outboard of the middle vertical support. Figure 1 illustrates the relative position of the tube sections in the steam generator.

Figure 2 a-h documents the as-received condition of section 23B. Not shown in this series of photomacrographs is the bend induced during the removal process and the severe scarring of the hot leg end caused by the tools used to remove section 23B. Section 23B was deformed and securely locked into the first vertical support by build-up of corrosion products in the tube-to-support crevice and significant effort was required to free it after TIG cutting was completed.

A major crack, approximately 1-1/4 inch long, was present at the six o'clock position of section 23B between the two scallop bar locations. Other areas of smaller cracks were present at either end of the major cracks. In one of these areas (Figure 2d), the cracks were oriented at an angle of 45° relative to the axis of the tube. Deposits at the scallop bar locations, which made location of the scallop bar positions possible, are shown in Figure 2d. Deposits, especially in areas near the major crack, were very thin and generally were orange to brown in color. At the scallop bar locations, there were some white deposits also present in addition to the orange-brown deposits.

Outside of the area of the vertical support, the tube section was covered with a black, or copper-brown colored loosely adherent deposit overlying a white deposit. In some areas, these deposits had flaked off exposing bare and non-corroded material underneath.

Tube section 23C was also covered with a dual layer of black or copper-brown colored deposits overlying a layer of whitish deposits (Figure 2i). There were no obvious areas of corrosion visible in section 23C nor were there any areas of deformation except for the deformed ends resulting from the cutting operation.

In addition to photomacrographs, C-E also used video tape to document the as-received condition of tube sections 23B and 23C from tube L29R84.

Section 4.0

LABORATORY EDDY CURRENT TESTING

After receipt tube sections 23B and 23C were re-examined by ECT. For this examination, a bobbin probe and MIZ 12 ECT equipment calibrated using an inline calibration standard with mix frequencies of 400 and 100 kHz was used. The deformation of tube section 23B precluded the use of any other probes or techniques for examination of this tube section.

ECT testing with the bobbin probe clearly showed a 100 percent throughwall signal at the location of the major crack. One end of the defect signal was not clearly resolved because of probe interference at the torch cut area of the tube section.

Approximately 1/4 inch from the hot leg end of the major defect, a second OD initiated indication was present. The location of this signal corresponded to the location of the second area of cracking. A mechanical kink in section 23B, induced during tube removal, distorted the signals from this smaller defect, rendering depth estimates impossible.

Significant dent signals were present at the general location of the defects in section 23B. These signals could not be quantified due to bending of the tube during removal from the steam generator. Several small dings were seen along the remaining portion of the tube section. These were not observed within the steam generator and, consequently, were probably caused during tube removal from the steam generator.

No defect signals were present in tube section 23C.

Section 5.0

DIMENSIONAL MEASUREMENTS

Figure 3 gives results of dimensional measurements from the defect region. These measurements were taken before descaling, and as such include the thickness of residual deposits. The data indicate that the tube was ovalized with the major axis (6-12 o'clock) being elongated by 0.046-0.122 inch while the minor axis (3-9 o'clock) was compressed by 0.045-0.070 inch diametrically. Figure 4 illustrates qualitatively the degree of ovalization present in the area of the major defect in section 238.

Section 6.0

MATERIALS CHARACTERIZATION

6.1 SECTIONING

C-E sectioned tube sections 23B and 23C in accordance with Figure 5 to provide samples for both materials characterization and defect characterization. The objective of the materials characterization testing was to determine if tube L29R84 was typical of mill annealed Alloy 600 tubing.

6.2 MICROSTRUCTURE CHARACTERIZATION

Transverse sections of tube sections 23B and 23C were metallographically prepared for evaluation using a dual electrolytic etch procedure. In this procedure, an Alloy 600 sample is etched with nital to reveal grain boundaries and with orthophosphoric acid to reveal carbide distribution and location. This procedure is used because the more commonly used electrolytic oxalic acid etch may give misleading information on carbide presence and distribution.

Figure 6 shows typical photomicrographs of the microstructure of tube L29R84 after the nital etch and the orthophosphoric etch. The microstructure of tube L29R84 consisted of medium size grains with some grain boundary carbides and very few intragranular carbides. - The microstructure of tube L29R84 was nominal and a typical example of mill annealed Alloy 600 tubing.

6.3 MODIFIED HUEY TEST

One piece from each of 23B and 23C was cut and tested using the modified Huey procedure to evaluate the degree of sensitization of tube L29R84. In this test, specimens were exposed to boiling 25% nitric acid for 48 hours. After the exposure, the pieces were cleaned and weight loss determined. Mill annealed material typically exhibits weight losses of 0.5% or less, while sensitized material exhibits weight losses in excess of 5.0%.

The weight losses for pieces 23B and 23C were 0.103% and 0.128%, respectively. This result, coupled with the dual etch microstructure results, confirms that tube L29R84 was in the mill annealed condition.

6.4 CHEMICAL ANALYSIS

Two pieces of tube L29R84, one each from sections 23B and 23C, were obtained for bulk chemical analysis to verify that there were no anomolies in the chemical composition of the tube. Both sections were chemically decontaminated using a nitric-hydrofluoric acid solution prior to chemical analysis.

Results of the chemical analysis are given in Table I along with the specified composition from ASME SB-163 (the applicable commercial tubing specification). The data show that the chemical composition of tube L29R84 was typical of Alloy 600 steam generator tubing.

Section 7.0

DEFECT CHARACTERIZATION

Figure 5 shows how sections 23B and 23C were further sectioned to provide samples of the defects for characterization.

7.1 ANALYSIS OF MAJOR CRACK

One end of the large throughwall crack was mounted, polished and examined to determine crack morphology. Figure 7 includes typical photomicrographs of cracks at the end of the major fracture. The intergranular nature of the cracks is evident in these photomicrographs. In the as-polished sections, there were no indications of intergranular attack (IGA) on the tube surface between the stress corrosion cracks. This was subsequently confirmed by etching the specimen with glyceregia, or an etchant which is particularly sensitive to IGA in nickel base alloys. Discrete intergranular stress corrosion cracks were present.

One face of the fracture surface was chemically descaled to remove all surface deposits using the standard two step APAC procedure. Subsequently, the specimen was examined by scanning electron microscope (SEM) to determine the relative amounts of IGSCC and ductile failure area. Figure 8 is a low magnification optical photograph of the descaled crack surfaces.

Figure 9 is a low power scanning electron micrograph showing a relatively flat crack surface with a central ductile tear ridge running from the O.D. to the I.D. surface of the tube. There were also other areas of ductile failure along the I.D. of the tube.

Figure 10 shows a section of the crack surface from O.D. to I.D. In this area, the failure appeared to be complete intergranular with evidence of secondary cracking resulting from branching of the main crack as it progresses through the material. The absence of any ductile failure area suggests that in this area a

small throughwall defect (and low level primary to secondary leakage) existed prior to the final rupture that resulted in large scale leakage.

Figure 11 is a montage of two photomicrographs showing the crack surface from O.D. (on the left) to the I.D. of the tube. Here, also IGSCC appeared to have progressed completely through the tube wall prior to final failure.

Figures 12-14 show that, although IGSCC covered most of the crack surface, there were small areas of ductile failure, as expected. Figure 12 shows a tear ridge extending from the O.D. to the I.D. surface. Figure 13 is a higher magnification scanning electron micrograph more clearly showing the transition from IGSCC to ductile failure near the I.D. surface.

Figure 14 is a high magnification scanning electron micrograph that shows more clearly the intergranular nature of the crack and the presence of secondary cracking. Figure 16 also shows throughwall IGSCC in yet another area of the crack surface.

The SEM examination of the crack surface clearly showed that IGSCC was the prevalent failure mode. In relative terms, IGSCC covered approximately 95 percent of the crack surface with the remaining area being a ductile failure formed during the final fracture of the tube.

7.2 ANALYSIS OF SMALLER CRACKS

A transverse metallographic section passing through the area containing the smaller cracks oriented at 45° to the tube axis was also prepared. This section was cut, ground and polished, without the application of any water, to prevent the elution of chemical species from the partial throughwall cracks. It was anticipated that contaminant species could be trapped in the tight intergranular cracks or in deposits in the crack. This metallographic section was examined by both light microscopy and scanning electron microscopy in the as-polished condition.

Typical photomicrographs of cracks in this area are shown in Figure 17. Several discrete cracks, with no indications of IGA were present in this section. The

intergranular nature of the cracks is readily apparent in these photomicrographs. There were no obvious deposits present in most of the cracked area. There was, however, significant amounts of metallographic mounting material present in the larger cracks.

This same section was examined with an SEM supplemented with energy dispensive spectrometry to identify chemical species present. Numerous EDS analyses of crack tip regions were completed without positive identification of contaminant species.

Typical scanning electron micrographs and EDS analysis results of crack tip regions are shown in Figures 18-23. Elements identified by EDS analysis included Ni, Cr and Fe from the tube base metal; Si, probably from the grinding operations; and minor indications in one or more loctions of Cl, S, Cu, K, Ca, Mg, Al and Ti. X-ray mapping of selected areas showed no major concentrations in the cracks of any of these elements. Thus, the EDS results provided no strong conclusions about possible aggressive species that may have promoted the IGSCC.

Section 8.0

SCALE ANALYSIS

8.1 pH MEASUREMENTS

There were only minor deposits present on tube L29R84 after it was removed from the steam generator. The flushing action of the leak may have removed deposits that had accumulated during operation. Measurement of the pH of the deposits on the tube were attempted with drops of deionized water and litmus paper. The litmus paper was capable of detecting pH's in the range of 9-12, with different colors at each .5 pH unit. The paper registered no reading (below 9) when wetted by deionized water.

Some of the deposits were subsequently removed from the tube surface and crushed to form a slurry. When the pH of the slurry was checked, no change in color of the litmus paper was registered. This suggests the pH was below 9.0.

Finally, drops of water were placed at several locations along section 23B. In general the pH paper did not register any color change at these locations. However, one spot along section 23B did have a color change, suggesting a pH of 10.0.

8.2 ANALYSIS OF SCRAPINGS

Scraping of the deposits from tube L29R84 were removed from the thin deposits in the scallop bar region and from the free length of tubing between vertical support straps. Deposit scrapings were dissolved in deionized water to facilitate analyses by ion chromatography and atomic absorption techniques. Ion chromatography detected 1793 ppm of SO_4 and 833 ppm of NO_3 in these deposits (error in measurement is $\pm$ 50%, due to the small sample size). Atomic absorption techniques did not detect metal cations such as potassium, sodium, calcium, or magnessium.

Outside the scallop bar vertical strap region, the dark flakes of deposit were analyzed for these same elements, and 147 ppm SO_4 and 78 ppm NO_3 were found. The concentration of potassium, sodium, calcium, and magnesium were below the 50 ppm detectability level for these relatively abundant scale deposits.

Scrapings were taken from the whitish colored deposits of the inner scale. They were collected from the various holes of the exterior scale at the 5:30 to 6:30 position away from the vertical strip-scallop bar region. When analyzed, 3256 ppm sulfate and 1500 ppm nitrate were observed. The error for this measurement was again estimated at $\pm$ 50%. No alkaline metals were detected. The above scale analysis for this tube L29R84 are summarized in Table II.

Section 9.0

DISCUSSION

OD initiated IGSCC has been identified as the cause of the steam generator tube failure at Ft. Calhoun. The elements required for IGSCC include (a) a susceptible material conditions, (b) a significant tensile stress, and (c) an aggressive environment. All elements must be present for IGSCC to occur.

Stress corrosion cracking (SCC) of Alloy 600 will occur under the appropriate condition in all metallurgical conditions, including the "mill annealed" condition. Material used in the steam generator tubes at Ft. Calhoun is typical of high temperature mill annealed Alloy 600. This material is resistant to IGSCC in some but not all environments.

Normal operating stresses in straight lengths of steam generator tubes are relatively low. Additional stresses may be imposed through support-tube interactions. At Ft. Calhoun, there was evidence that the failed tube was constrained by the vertical support strips to the extent that deformation of the tube occurred, probably the result of indigenous corrosion product growth on the vertical support. This lateral deformation provided additional stress at the point where failure occurred.

Three different environments are known to be capable of producing IGSCC in Alloy 600. These environments are (a) caustic (caustic stress corrosion cracking), (b) relatively pure water (Coriou stress corrosion cracking), and (c) sulfur containing environments. Of these environments, C-E considers that a caustic environment was the most likely cause of the observed failure.

A caustic environment may have occurred in steam blanketed areas at Ft. Calhoun as a result of periodic low level condenser in-leakage. When concentrated, the cooling water (Missouri River) tends to become alkaline, thereby producing a caustic condition. Deposits in the steam blanketed area, which may have contained alkaline species such as Na, K, etc., may have redissolved during the

plant shutdown prior to the failure. This could explain the absence of these elements in the small cracks adjacent to the failure. Although some deformation of the tube occurred during service, the total deformation was relatively small (less than one percent). Caustic SCC has been produced in the laboratory in Alloy 600 at strain levels as low as 0.5% (elastic plus plastic). Also, caustic SCC has occurred in relatively short times at temperatures of $600^\circ F$ or less, which approximates the tube wall temperature at Ft. Calhoun. These observations, coupled with the fact that the failures occurred in a steam blanketed area where caustic species could concentrate, leads C-E to conclude that the failure was probably the result of caustic stress corrosion cracking.

Pure water stress corrosion cracking (Coriou cracking) is considered as a significantly less probable mechanism for the tube failure. Coriou cracking has been identified as the failure mechanism in numerous steam generator tube failures in both domestic and foreign PWRs. No chemical contaminant(s) have been associated with this type of SCC. Field and laboratory failures attributed to this particular mechanism generally occur in either highly deformed tubes (strains greater than 14%) or in tubes with distinct mechanical and/or microstructural characteristics (high strength and intragranular carbides). Most, although not all, of the Coriou type failures have been I.D. initiated.

Although the failure tube at Ft. Calhoun was deformed, the total strain was relatively low (less than one percent). Furthermore, the tubing used at Ft. Calhoun was relatively low strength and the microstructure appeared relatively resistant to Coriou cracking, i.e., intergranular carbides with few intragranular carbides. Similar tubing has been severely deformed as a result of support plate and/or eggcrate denting in other C-E supplied steam generators. Non-destructive and post-service destructive examinations of removed tubes have confirmed the absence of Coriou type cracking in these steam generators. Furthermore, Coriou cracking is strongly temperature dependent and thus tends to occur when temperature is the highest; i.e., on the tube I.D. The Ft. Calhoun failure was O.D. initiated.

Based on these observations, Coriou cracking is not considered to be the cause of the Ft. Calhoun tube failure.

IGSCC induced by a sulfur containing compound is the least likely of the three

postulated failure mechanisms. There was no apparent source of S bearing compounds at Ft. Calhoun, other than the condenser cooling water. Furthermore, the condenser cooling water becomes alkaline when concentrated, not acidic. The various forms of S induced corrosion (IGSCC, wastage, intergranular attack, pitting) all occur at acidic values of pH. In addition, analysis of the intergranular cracks in the failed tube did not produce evidence of the presence of S, although some S compounds (ex. NiS) that form in high temperature aqueous environments are insoluble.

Section 10.0

CONCLUSIONS

The detailed examination of section of tube L29R84 from the Ft. Calhoun "B" steam generator resulted in the following conclusions/findings:

1. The cause of the failure of tube L29R84 was intergranular stress corrosion cracking which propagated essentially throughwall during the preceeding fuel cycle. During plant heat-up at the start of the next cycle, the remaining uncracked portion of the tube failed as a result of a ductile overload.

2. The major crack was located on the bottom of the tube between the scallop bars in the first (hot leg) vertical support strap.

3. The tube had been ovalized as a result of corrosion product build-up in the tube-to-support crevice.

4. The most likely mechanism of failure was caustic stress corrosion cracking with the caustic environment being developed by the concentration of in-leakage of the condenser cooling water.

5. Tube L29R84 was typical of mill annealed Alloy 600 tubing used in C-E supplied steam generators. The chemical composition, microstructure and degree of sensitization were all nominal for mill annealed Alloy 600.

Table I

CHEMICAL COMPOSITION OF TUBE L29R84

Ni	Cr	Fe	Mn	Cu	Si	C	S	Co	
72.0 (min)	14.00-17.00	6.00-10.00	1.0 (max)	0.5 (max)	0.5 (max)	0.15 (max)	0.015 (max)	-	SB-163
76.08	14.50	8.16	0.248	0.325	0.190	0.025	0.001	0.035	23B
76.04	14.44	8.26	0.245	0.324	0.195	0.024	0.001	0.035	23C

Table II

SCALE ANALYSIS FROM TUBE L29R84
(In ppm, based on original dry weight of scale)

SCALE SCRAPINGS	SO$_4$	NO$_3$	K, Na, Ca, Mg
Scallop Bar Region	1793*	833*	1050
Dark Exterior Scale Outside Scallop Bar Area	147	78	50
Whitish Deposits Within Holes of Dark Exterior Scale	3256*	1500*	2500

*Values are ± 50%

Table 1

ELEMENTAL ANALYSIS

Ni	Cr	Fe	Mn	Cu	Si	C	S	Co	
72.0 (min)	14.00-17.00	6.00-10.00	1.0 (max)	0.5 (max)	0.5 (max)	0.15 (max)	0.015 (max)	-	SB-163
76.08	14.50	8.16	0.248	0.325	0.190	0.025	0.001	0.035	23B
76.04	14.44	8.26	0.245	0.324	0.195	0.024	0.001	0.035	23C

Figure 1. Location of Tube Sections 23B and 23C of Tube L29R84 in the B Steam Generator.
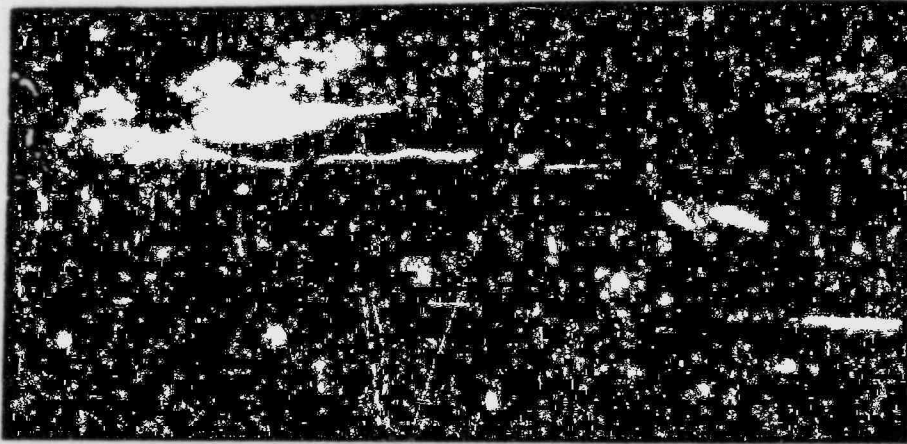
(a) Overall View of the Major Crack
(Neg. #68014, 2X)
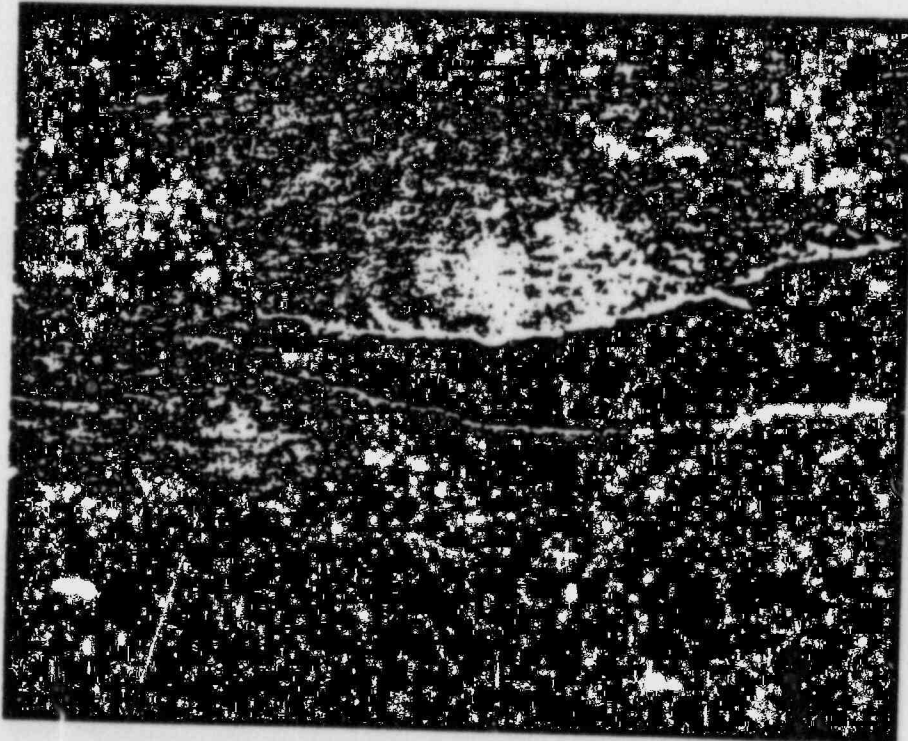
(b) Close-up View of One End of the Major Crack
(Neg. #68015, 8X)

Figure 2. Photomacrographs Documenting the As-Received Condition of Tube L29R84.

(c) Bottom Scallop Bar Location in Section 23B
     (Neg. #68010, 1.5X)
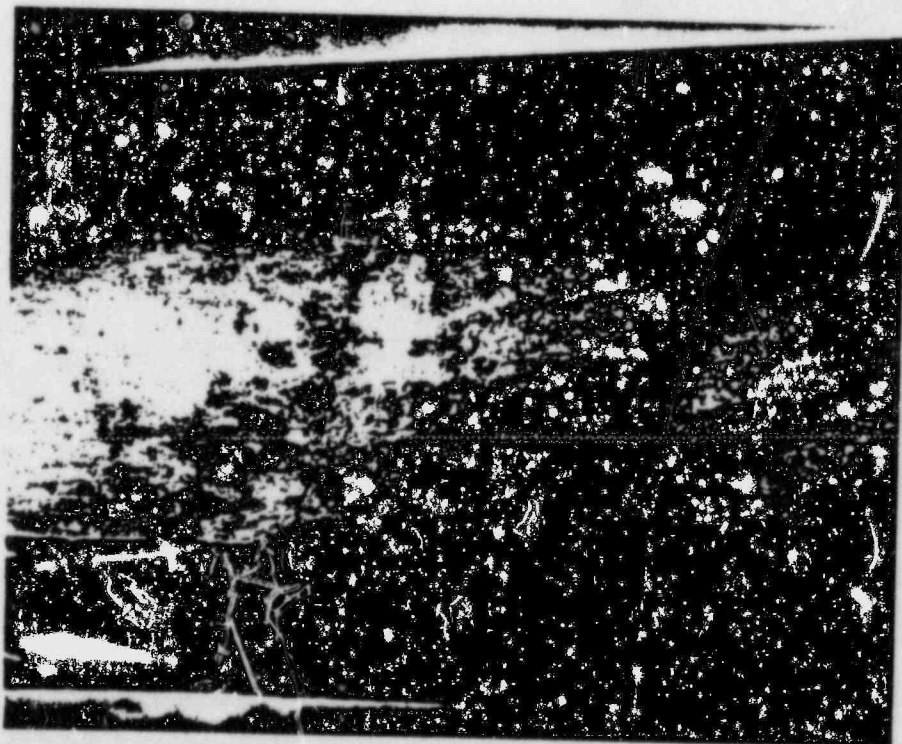
(d) Area of Smaller Cracks Oriented 45° to Tube Axis
     (Neg. #68011, 5X)

Figure 2. Photomacrographs Documenting the As-Received Condition of
           Tube L29R84 (continued).
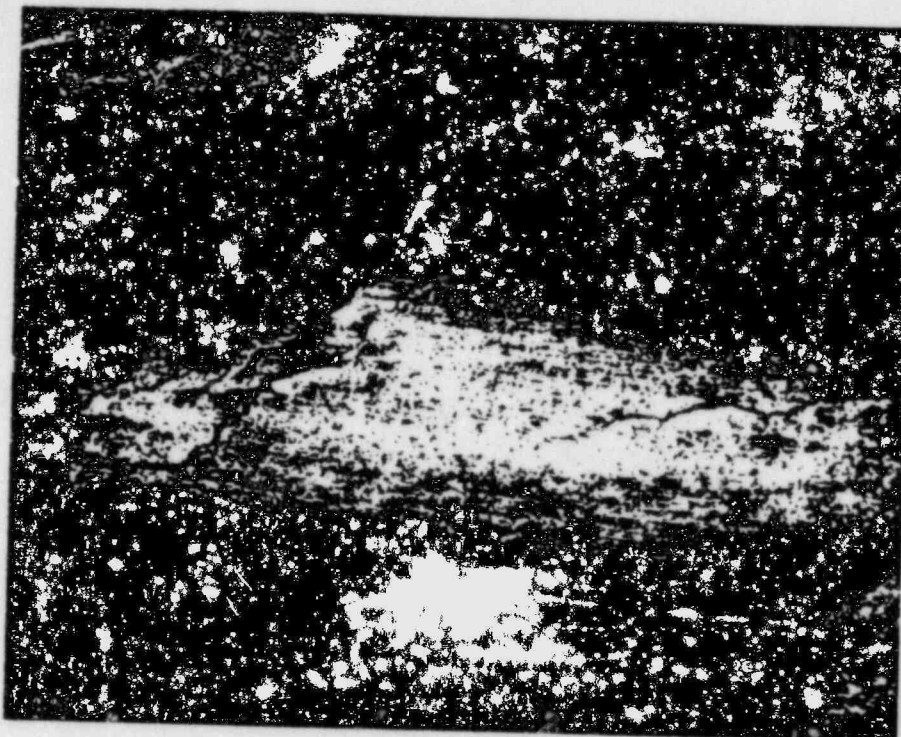
(e) Close-Up View of the Area of Smaller Cracks
(Neg. #68106, 20X)

(f) Top Scallop Bar Location of Section 23B
(Neg. #68012, 2X)

Figure 2. Photomacrographs Documenting the As-Received Condition of
Tube L29R84 (continued).

(g) Area of Deposits on Section 23B
(Neg. #68013, 2X)

(h) View of the Fracture Surface of the Major Crack
(Neg. #68008, 20X)

Figure 2. Photomacrographs Documenting the As-Received Condition of Tube L29R84 (continued).
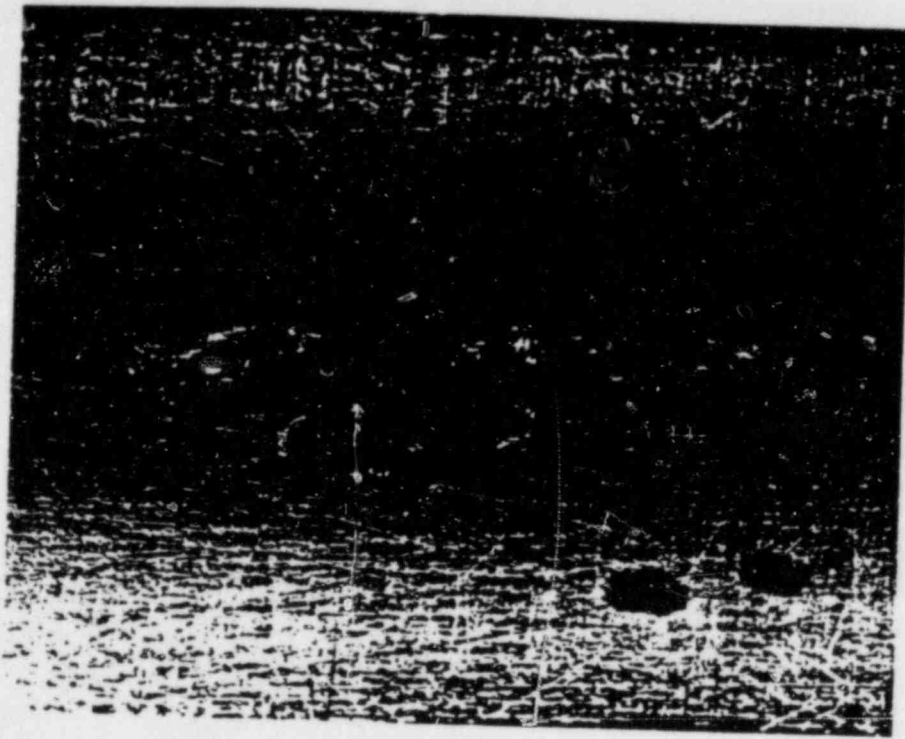
(i) Area of Deposits on Section 23B
     (Neg. #68013, 2X)

Figure 2. Photomacrographs Documenting the As-Received Condition of
Tube L29R84 (continued).
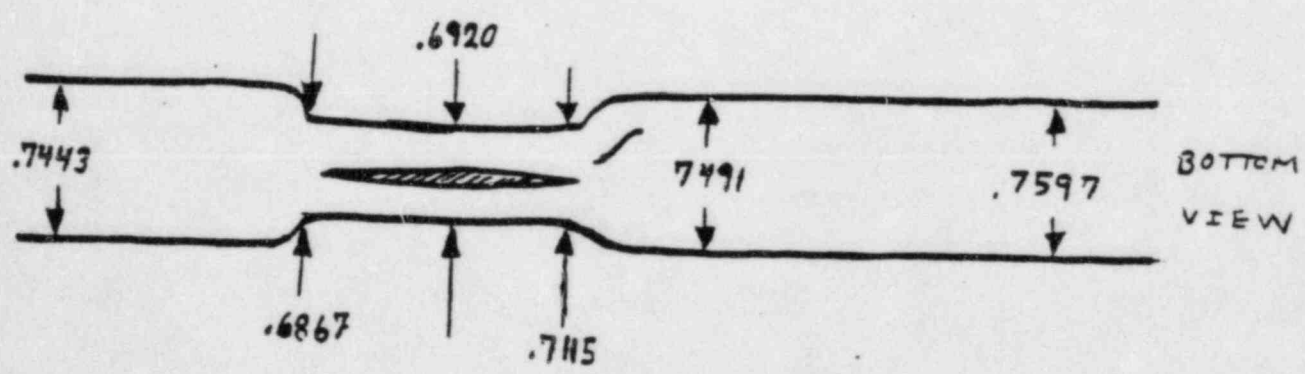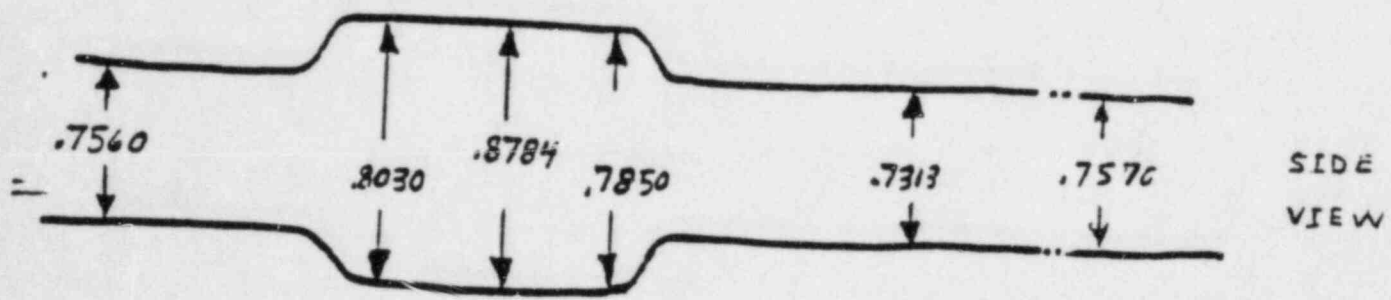
Figure 3. Dimensional Measurements of Section 23B.

Figure 4. Cross-Section View of Tube Section 23B Near the Major Crack Showing Extent of Service Induced Ovalization. (Neg. #68026, 3X)
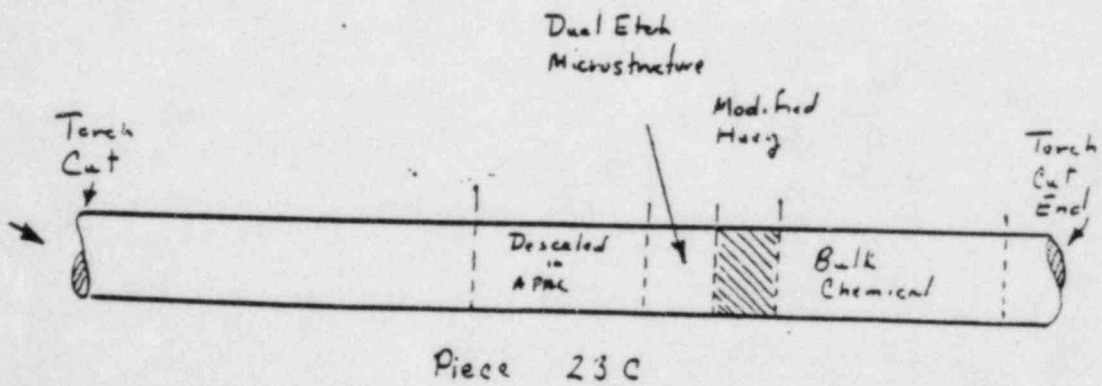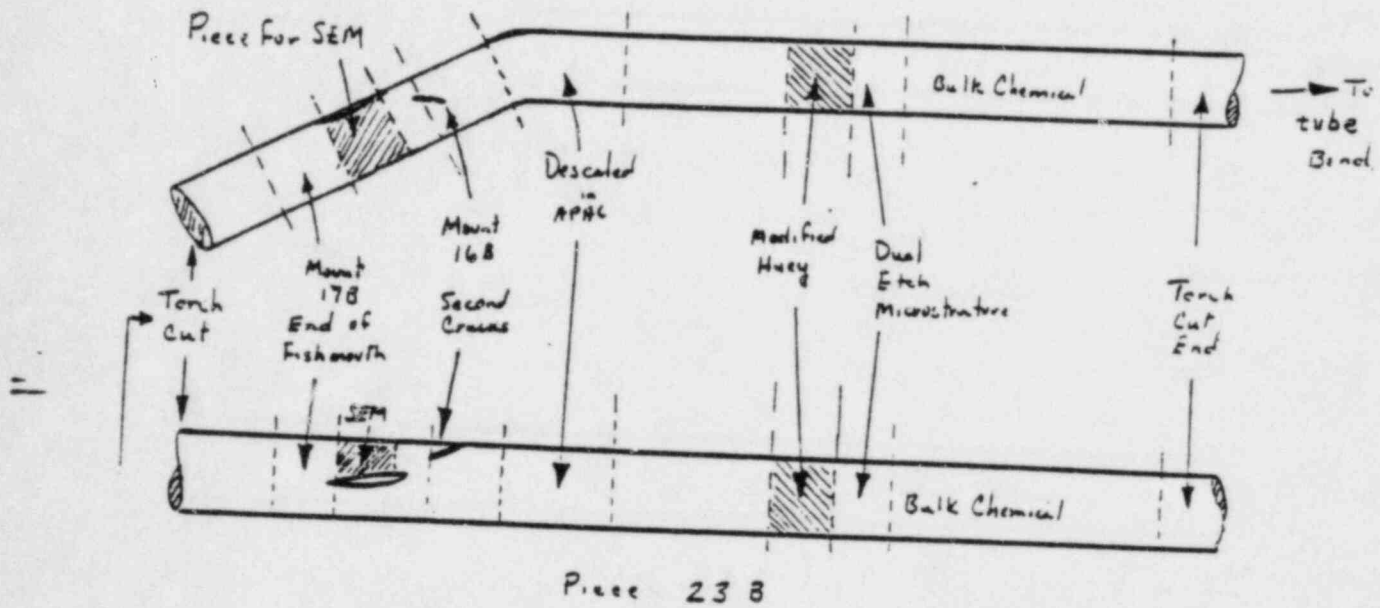
Figure 5. Sectioning Diagram Showing the Location of Samples Removed
for Various Analyses.
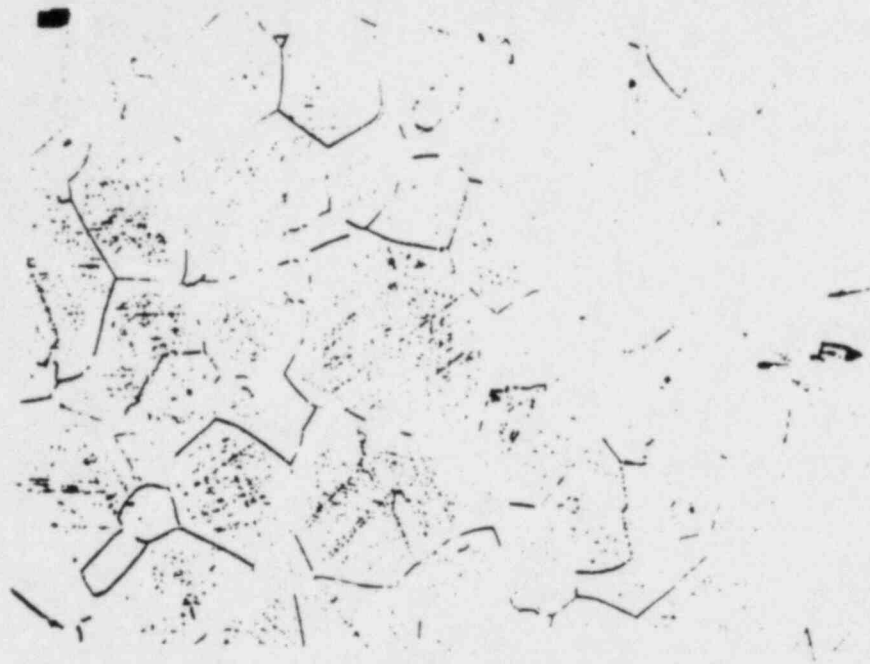
Nital Etch
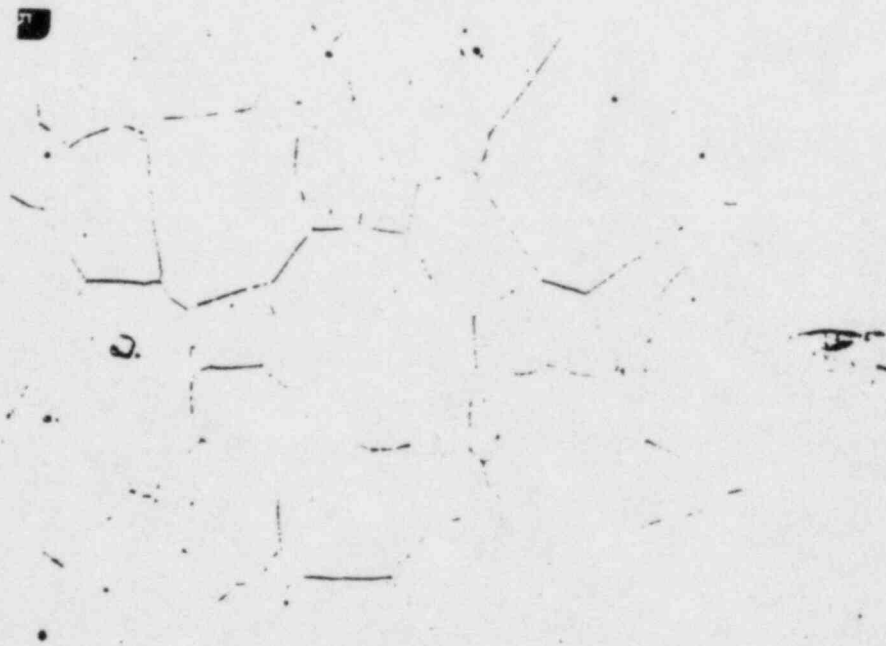
Orthophosphoric Etch

Figure 6. Microstructures of Tube L29R84 (Transverse View, Neg.
#68020, 68021, 500X).

(a) As-Polished (Neg. #68022, 200X)

(b) Higher Magnification View of a Crack Shown in Figure 7a
(Nital Etch, Neg. #68017, 500X)

Figure 7. Transverse View of Cracks at the End of the Major Crack, Mount 17B.
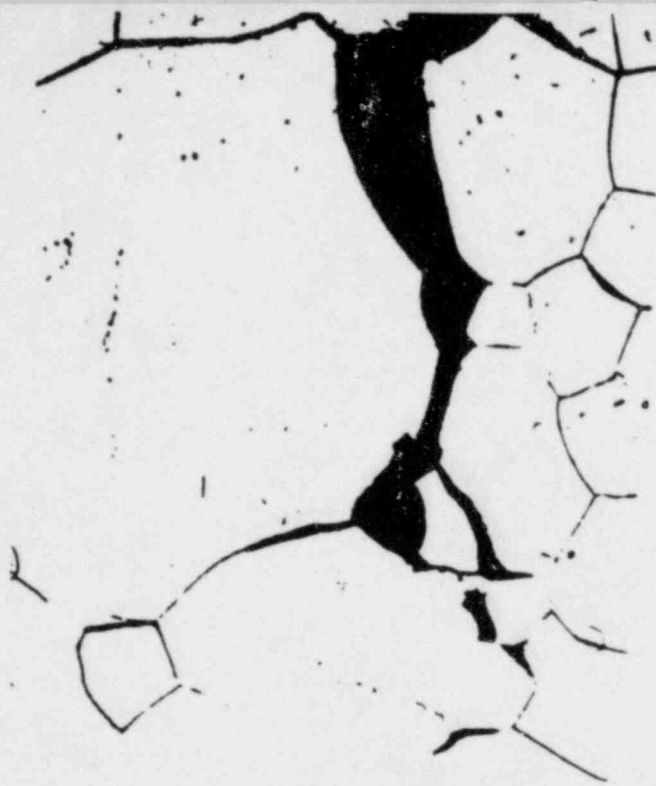
(c) Tip of One of the Figure 7a Cracks
(Nital Etch, Neg. #68018, 1000X)
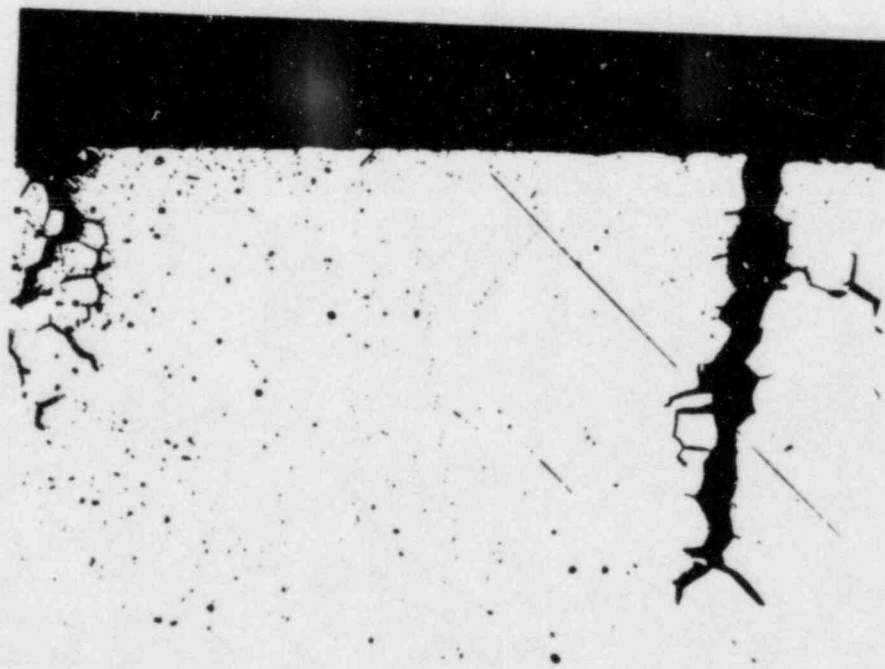
(d) Area Shown in Figure 7a After Etching with
Glyceregla to Determine if Intergranular Attack
Had Occurred.
(Neg. #68059, 200X)

Figure 7. Transverse View of Cracks at the End of the Major Crack,
Mount 17B (continued).
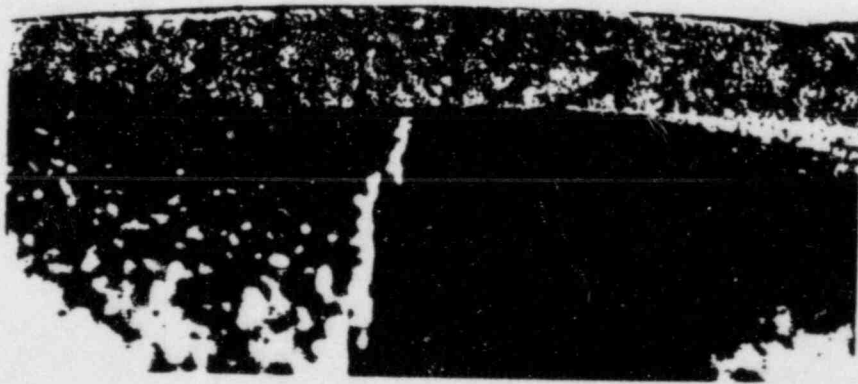
Figure 8. A Section of the Major Crack After Descaling for Scanning
Electron Microscope Examination.
(Neg. #68025, 10X)
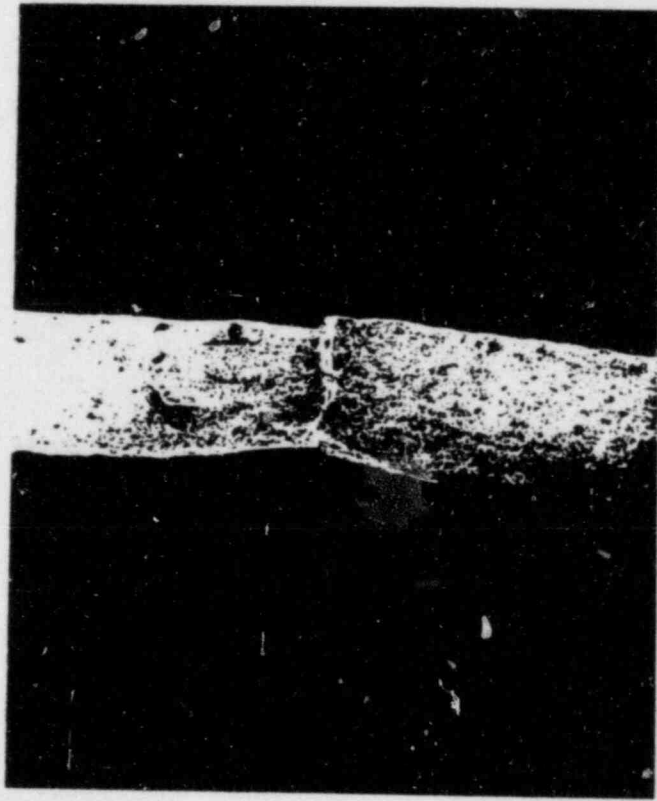
Figure 9. Low Power Scanning Electron Micrograph of the Fracture
Surface.
(Neg. #68039, 10X)
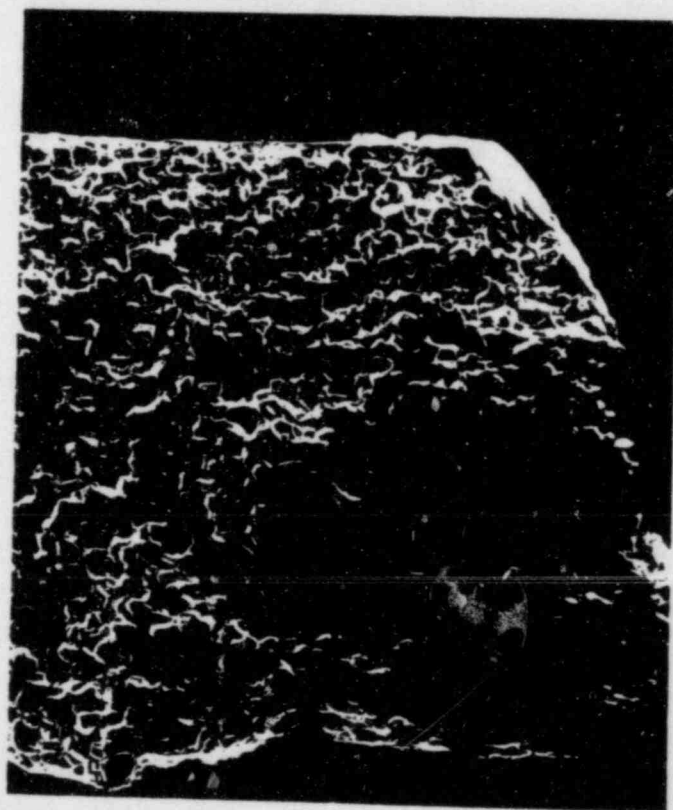
Figure 10. Scanning Electron Micrograph Showing Appearance of the
Fracture Surface from O.D. to I.D.
(Neg. #68045, 70X)
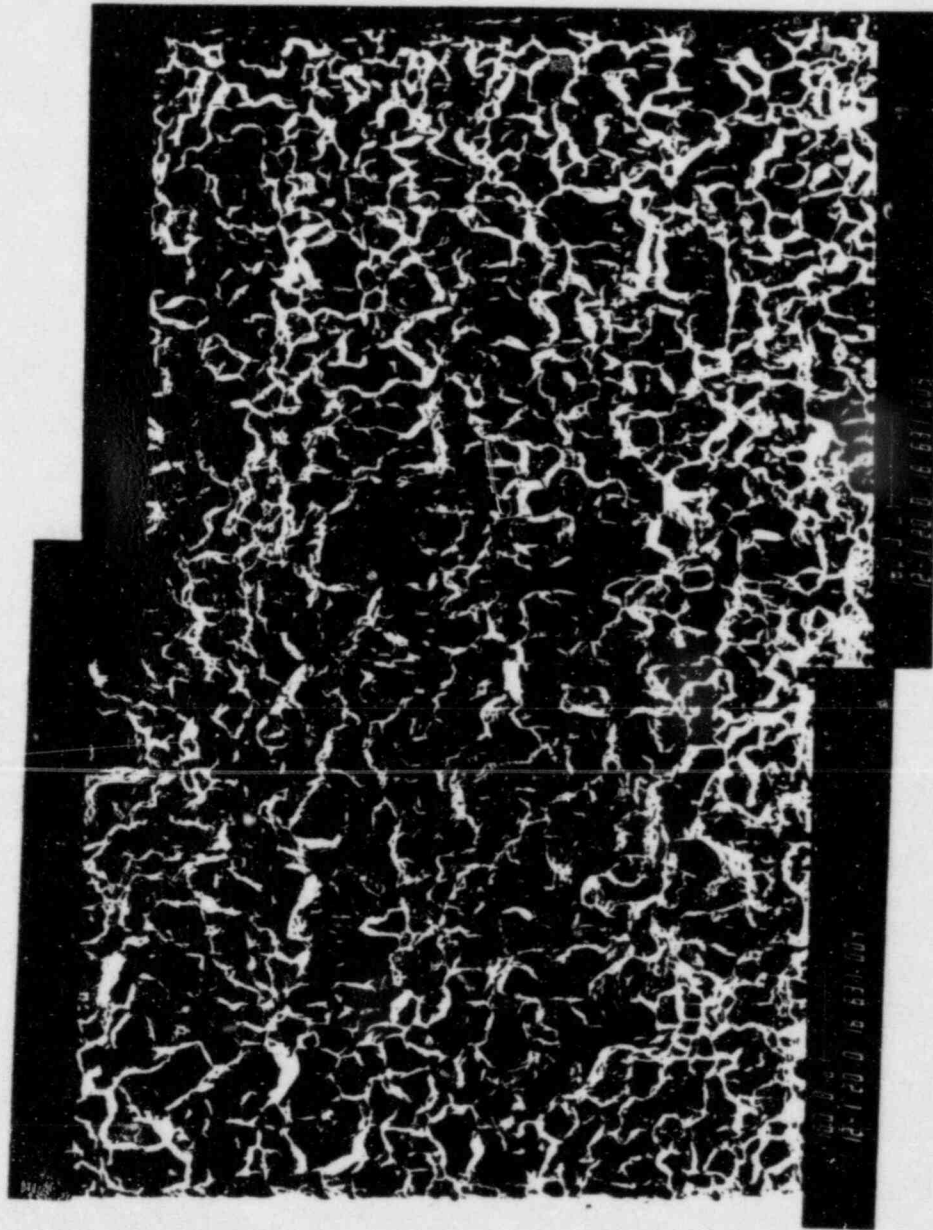
Figure 11. Montage of Scanning Electron Micrographs Showing the Appearance of the Crack Surface of the Major Crack.
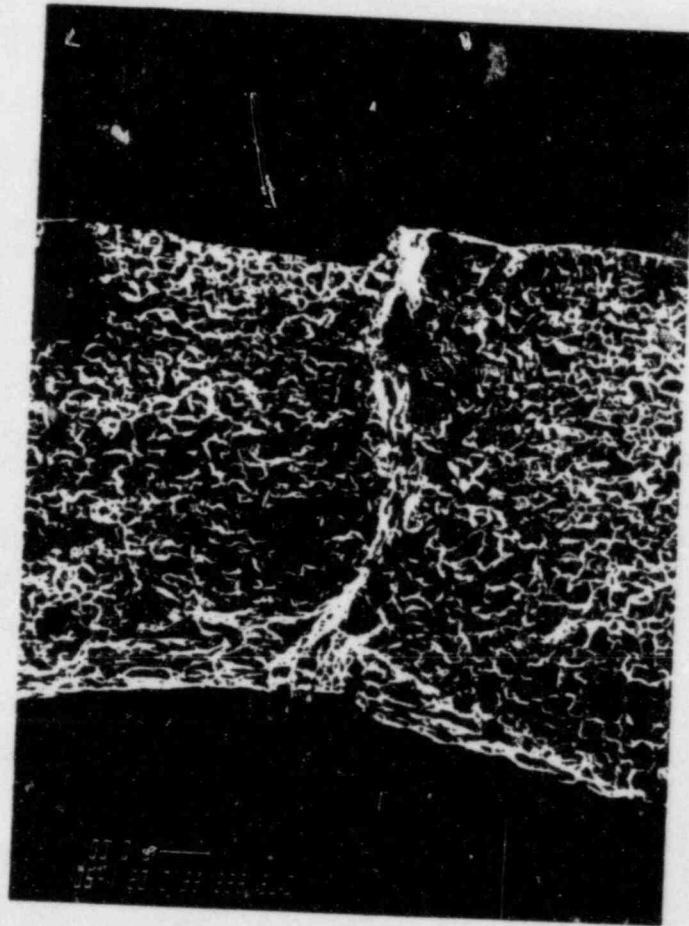
Figure 12. Scanning Electron Micrograph Showing a Ductile Tear Ridge
Extending from O.D. to I.D. Surface.
(Neg. #68034, 60X)
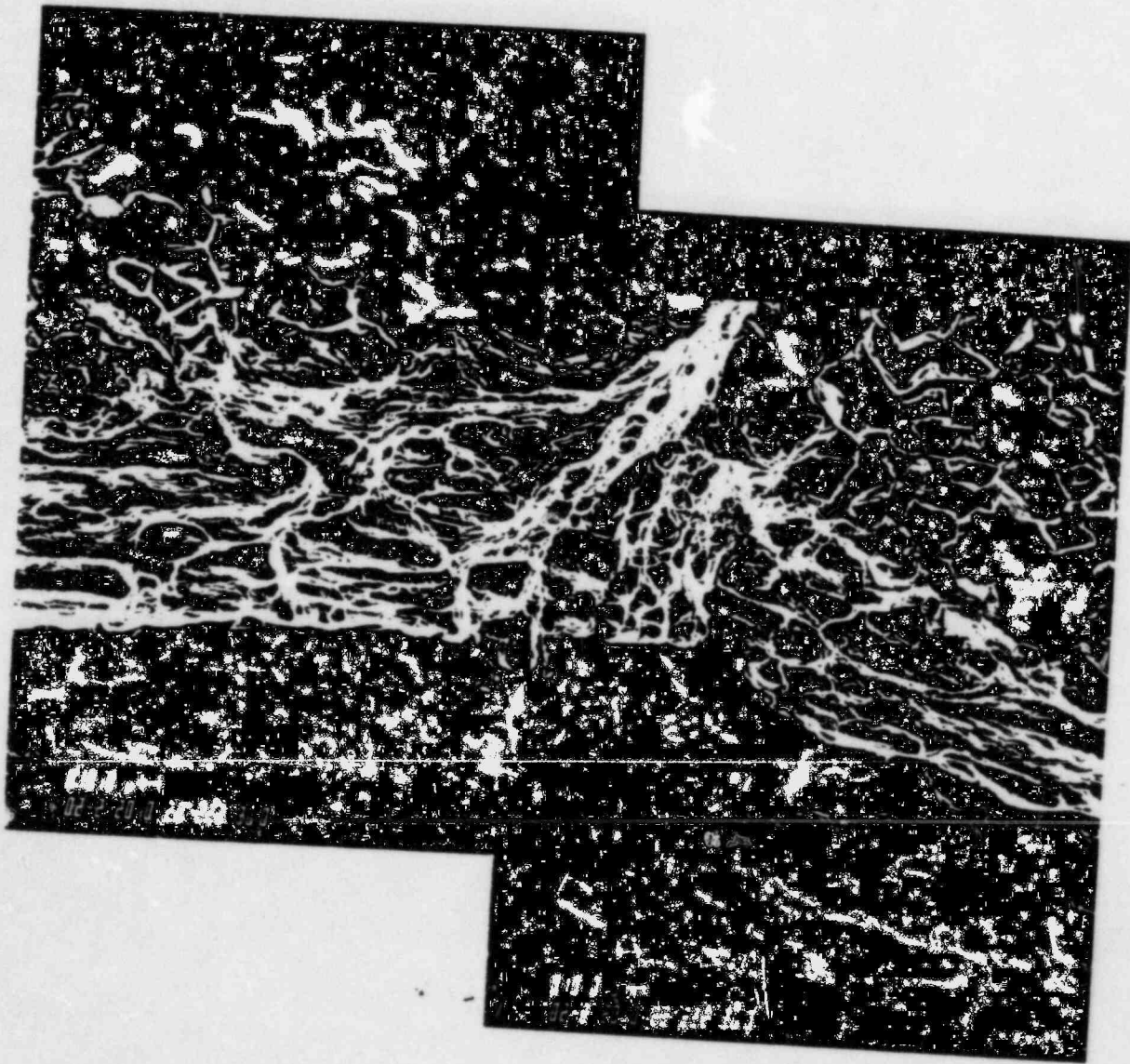
Figure 13. Scanning Electron Micrographs Showing Part of the Ductile
Tear Ridge Shown in Figure 12.
(Neg. #68033, 200X)

Figure 14. A Ductile Tear Area Surrounded on Both Sides by Areas of
Intergranular Cracking, Including Some Secondary Cracking.
(Neg. #68043, 150X)

Figure 15. High Magnification View of an Area of the Major Crack
Surface Showing Intergranular Nature of the Crack.
(Neg. #68046, 500X)
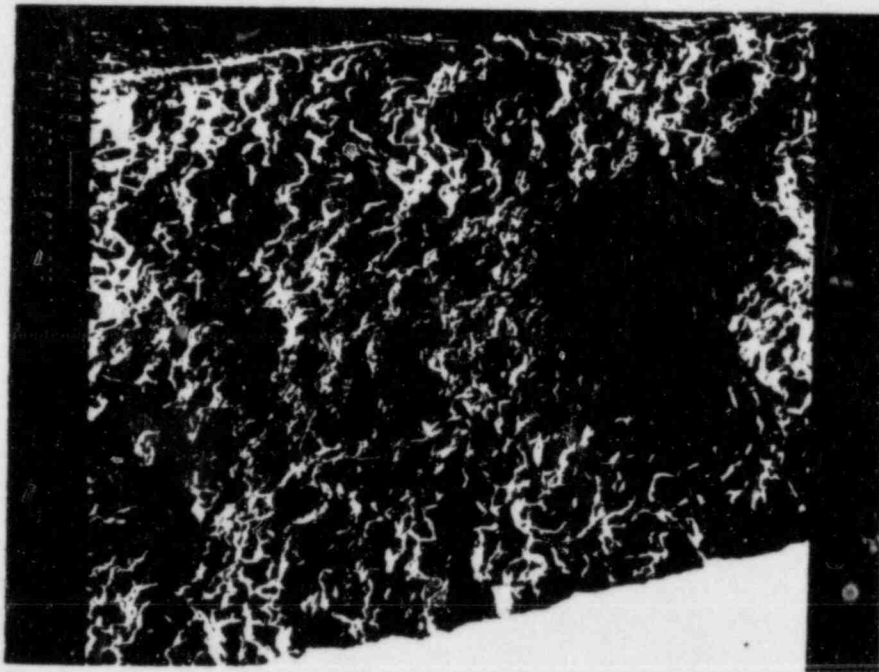
Figure 16. Scanning Electron Micrograph of Another Area of the Major
Crack Showing Intergranular Cracking from O.D. to I.D.
Surfaces.
(Neg. #68049, 70X)
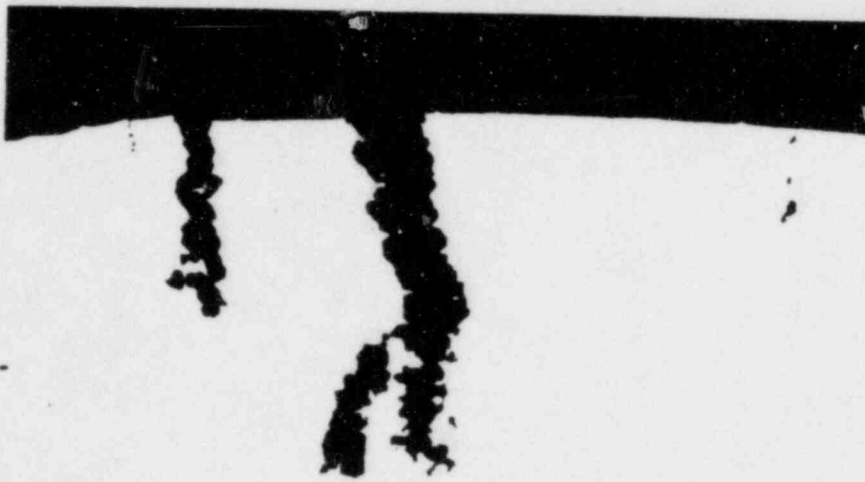
(a) (Neg. #68031, As-Polished, 50X)
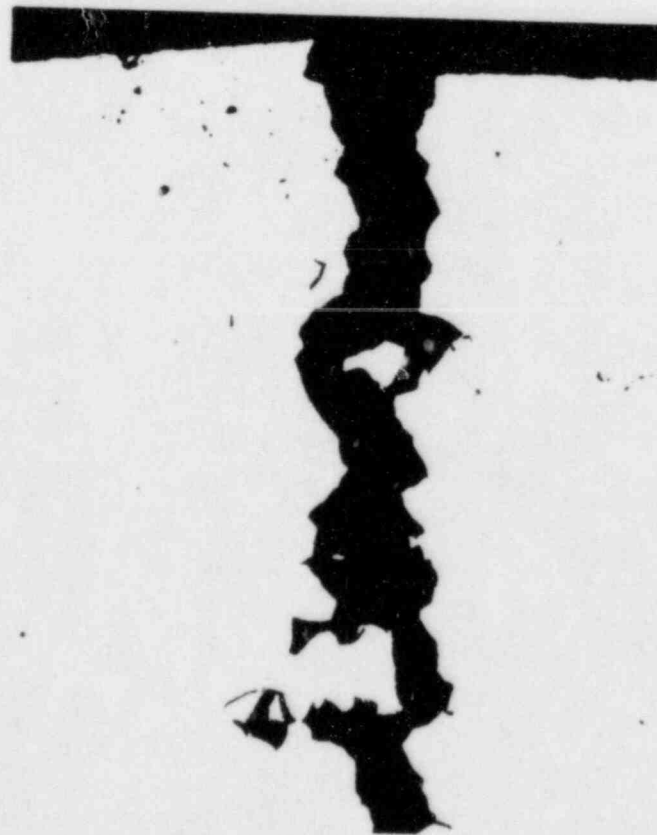
(b) (Neg. #68029, As-Polished, 200X)

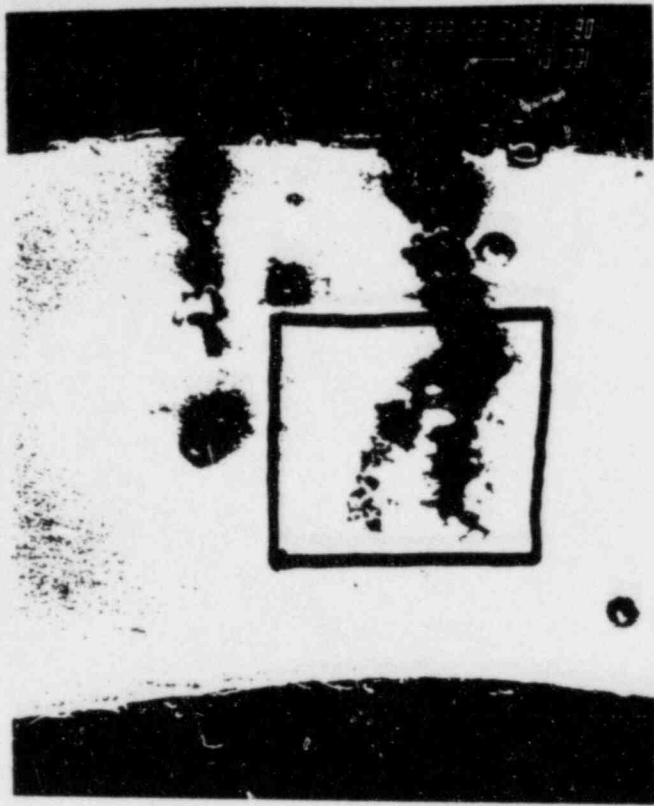Figure 17. Transverse View of Individual Cracks in the Smaller Area of Cracking.

(c) Higher Magnification View of the Deposit Crack in
Figure 17a.
(Neg. #68028, As-Polished, 500X)
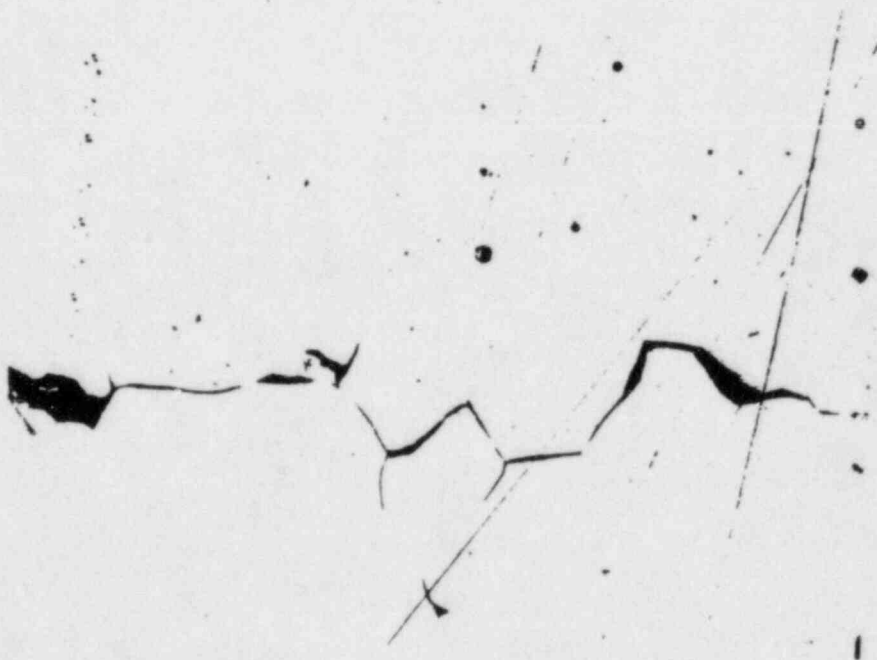
(b) High Magnification View of the Small Crack in
Figure 17a.
(Neg. #68030, As-Polished, 500X)

Figure 17. Transverse View of Individual Cracks in the Smaller Area of
Cracking (continued).

(c) Overall View
(Neg. #68036, 60X)

(b) Close-Up of Area Indicated
(Neg. #68037, 100X)

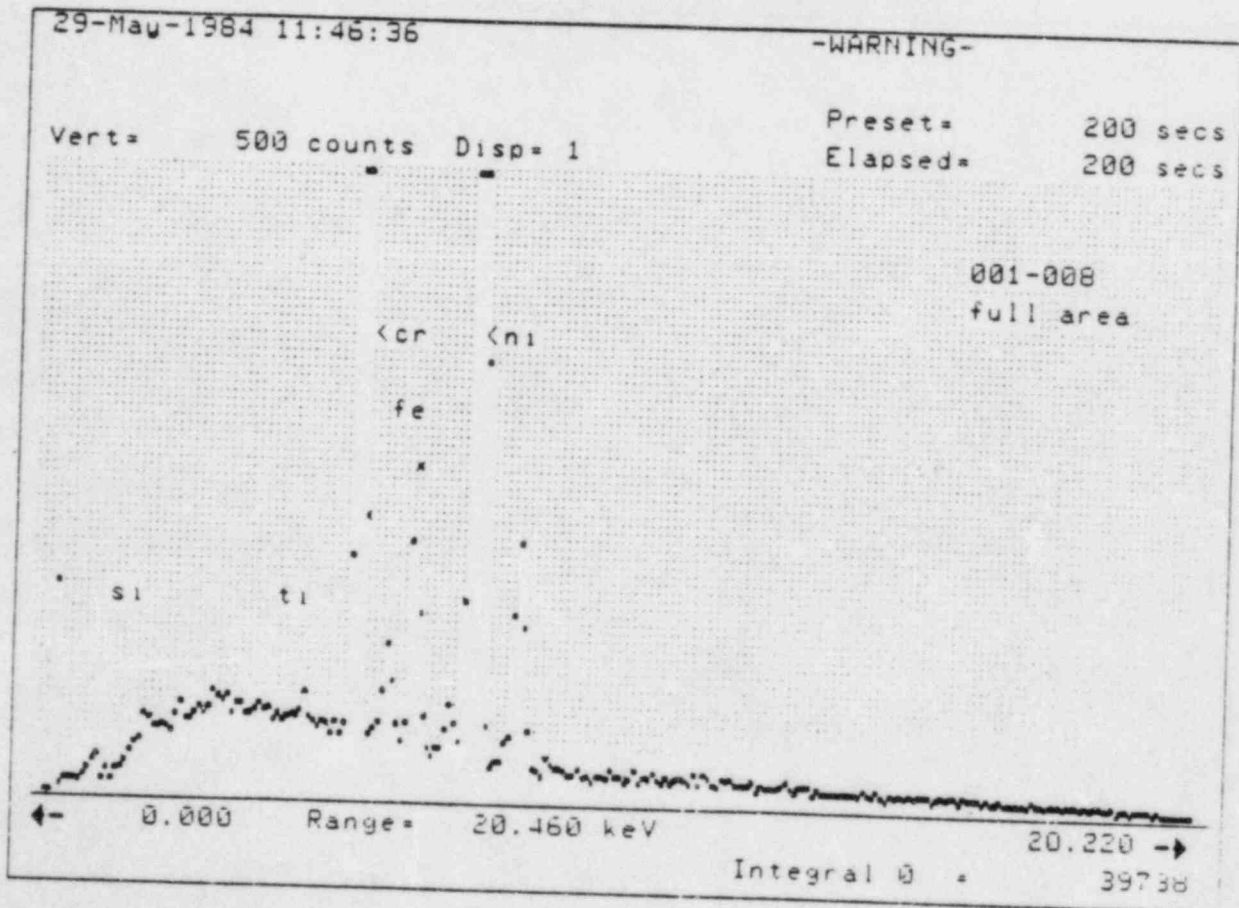Figure 18. Scanning Electron Micrographs of the Specimen Shown in Figure 18.

Figure 19. Scanning Electron Micrograph of Crack Tips and EDS Analysis
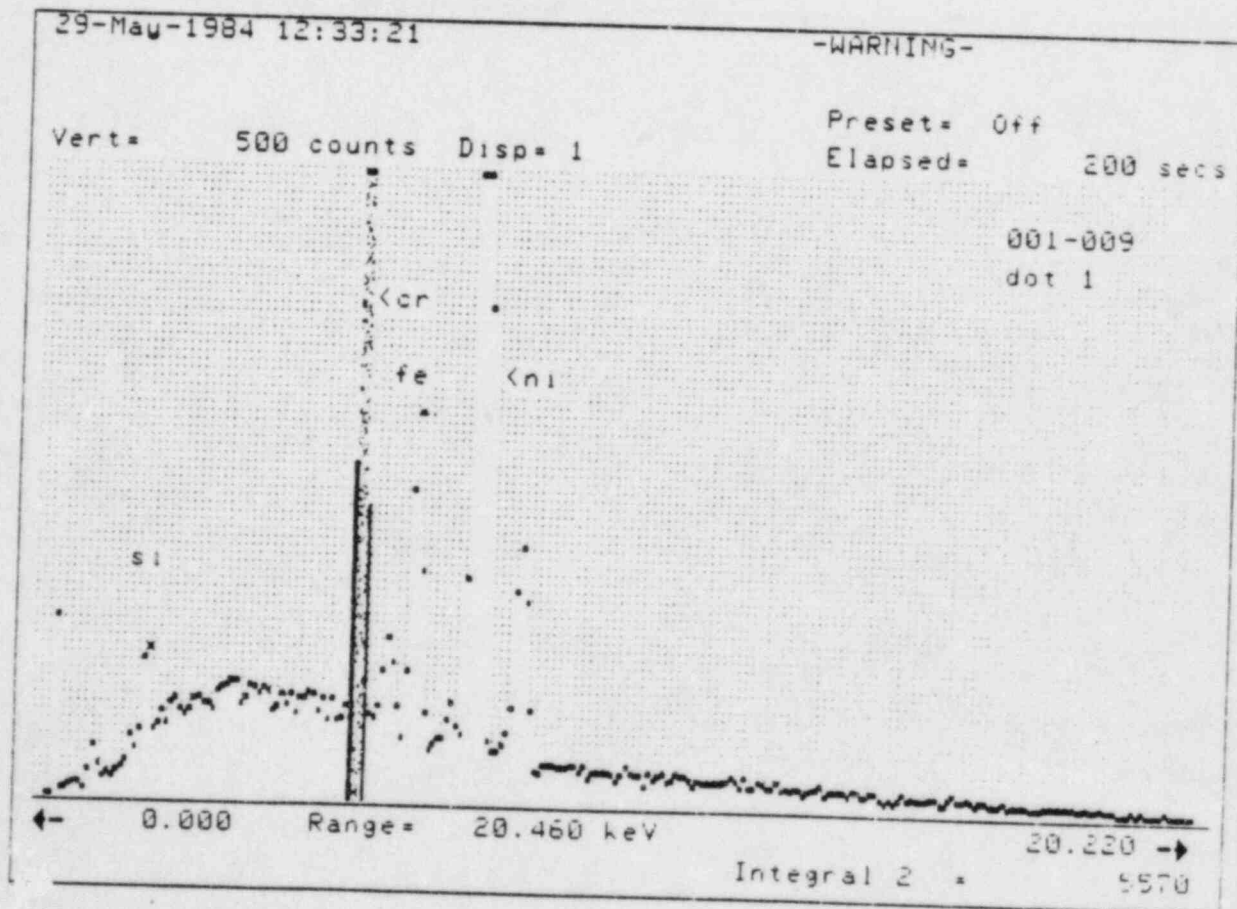Results from the Area Shown.
(Neg. #67771, 260X)

Figure 20. Scanning Electron Micrograph of Crack Tips and EDS Analysis
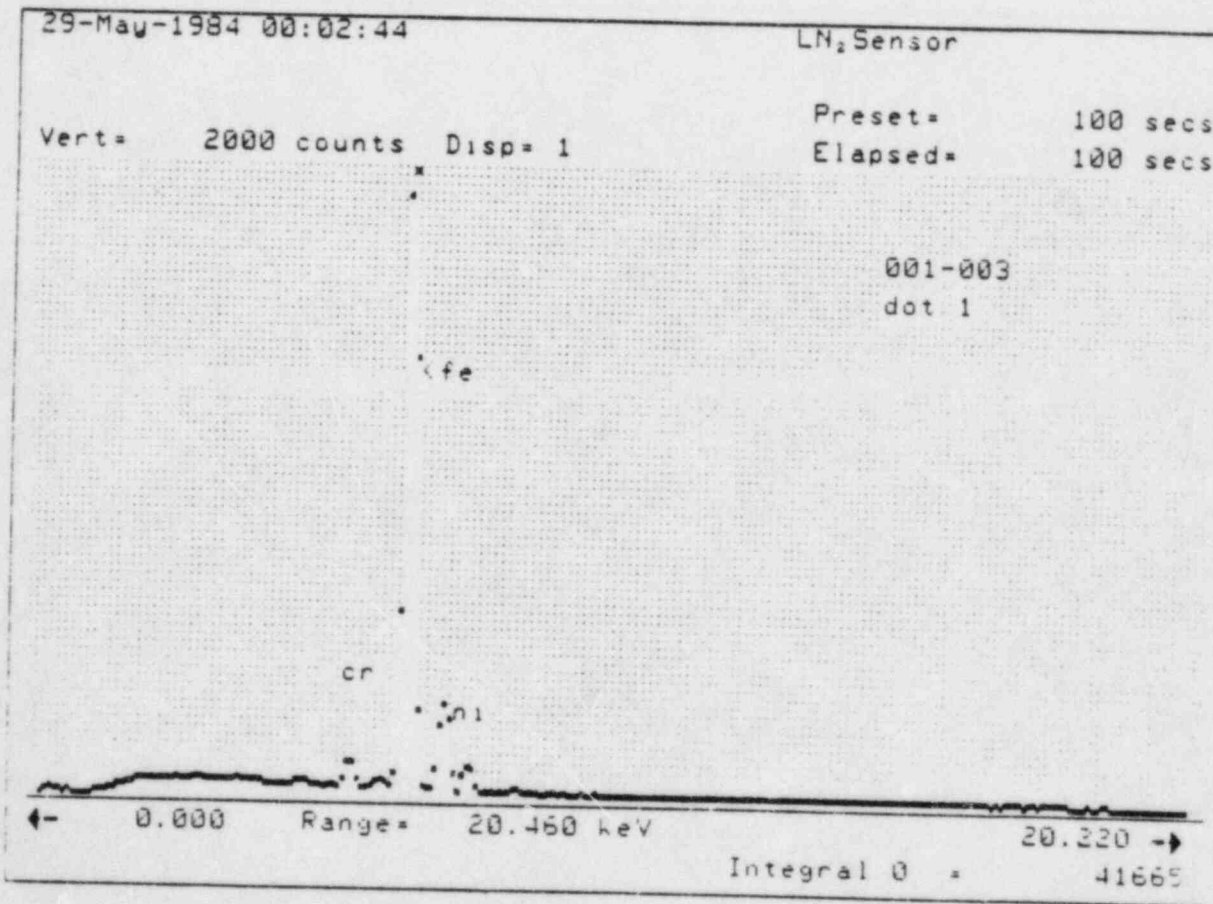Results from the Area Shown.
(Neg. #67772, 1500X)

29-May-1984 00:02:44   LN₂ Sensor

Vert =   2000 counts   Disp = 1   Preset =   100 secs
                                        Elapsed =   100 secs

                                              001-003
                                              dot 1

                fe

            cr
                 ni

     ◄—   0.000   Range =   20.460 keV   20.220 —►
                              Integral 0   =   41665

Figure 21. Scanning Electron Micrograph of Crack Tips and EDS Analysis
          Results from the Area Shown.
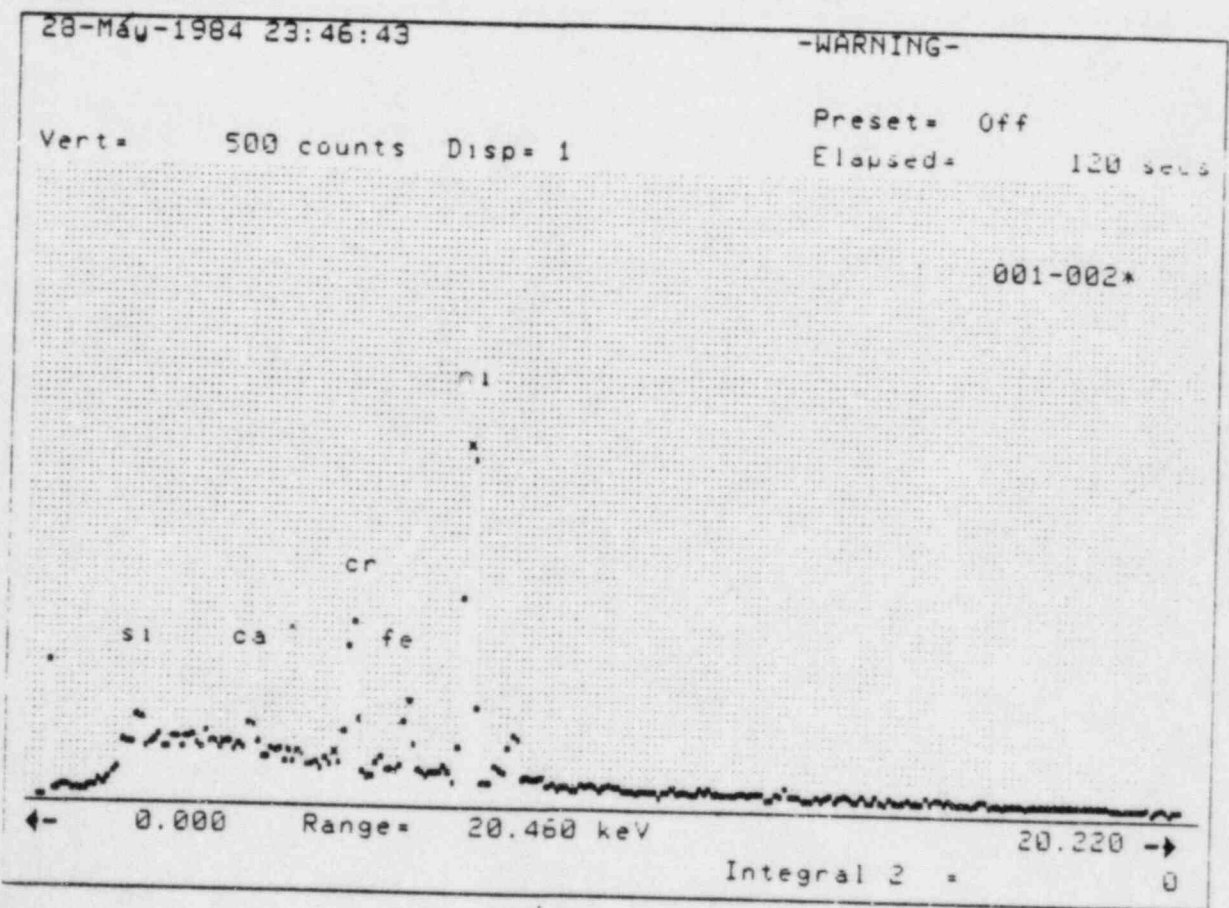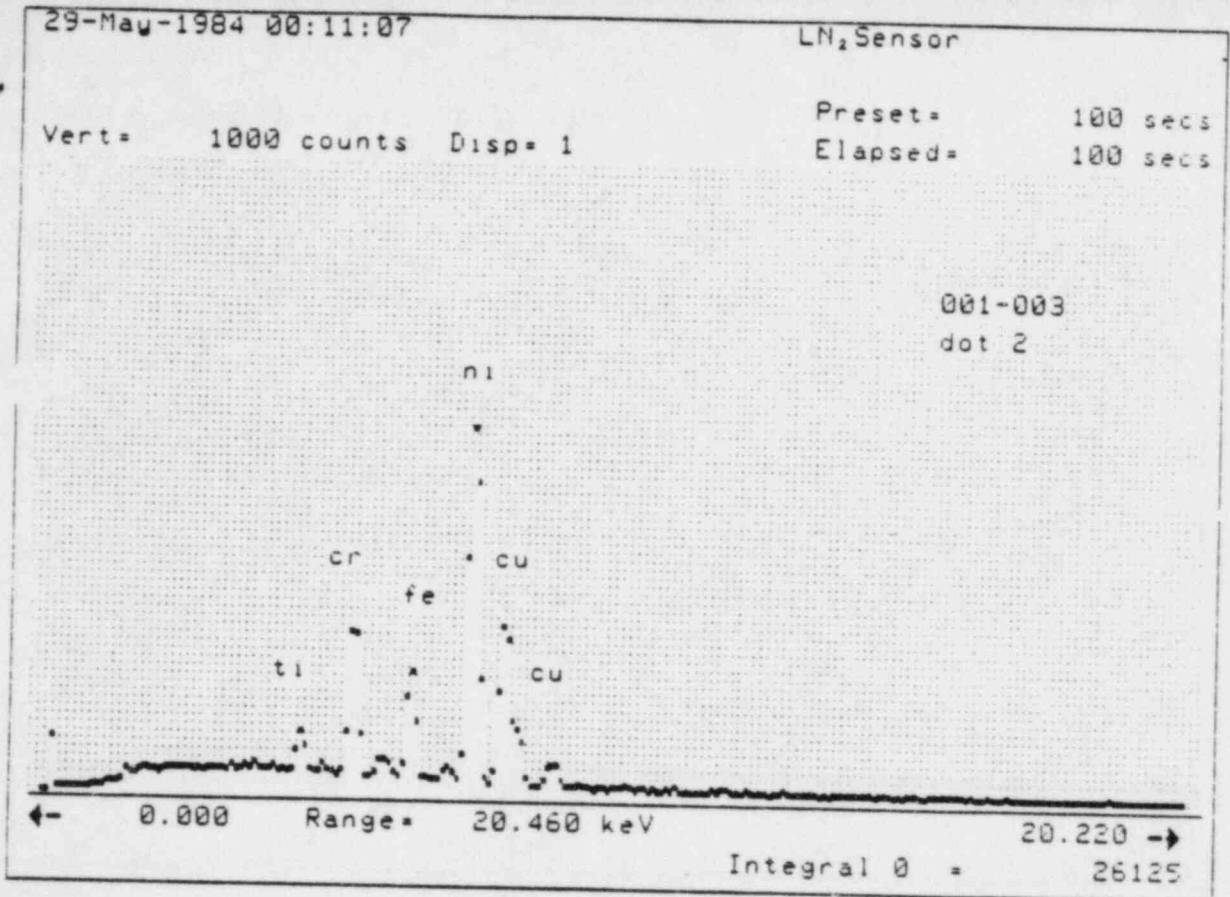   (Neg. #67769, 1000X)

Figure 21. Scanning Electron Micrograph of Crack Tips and EDS Analysis
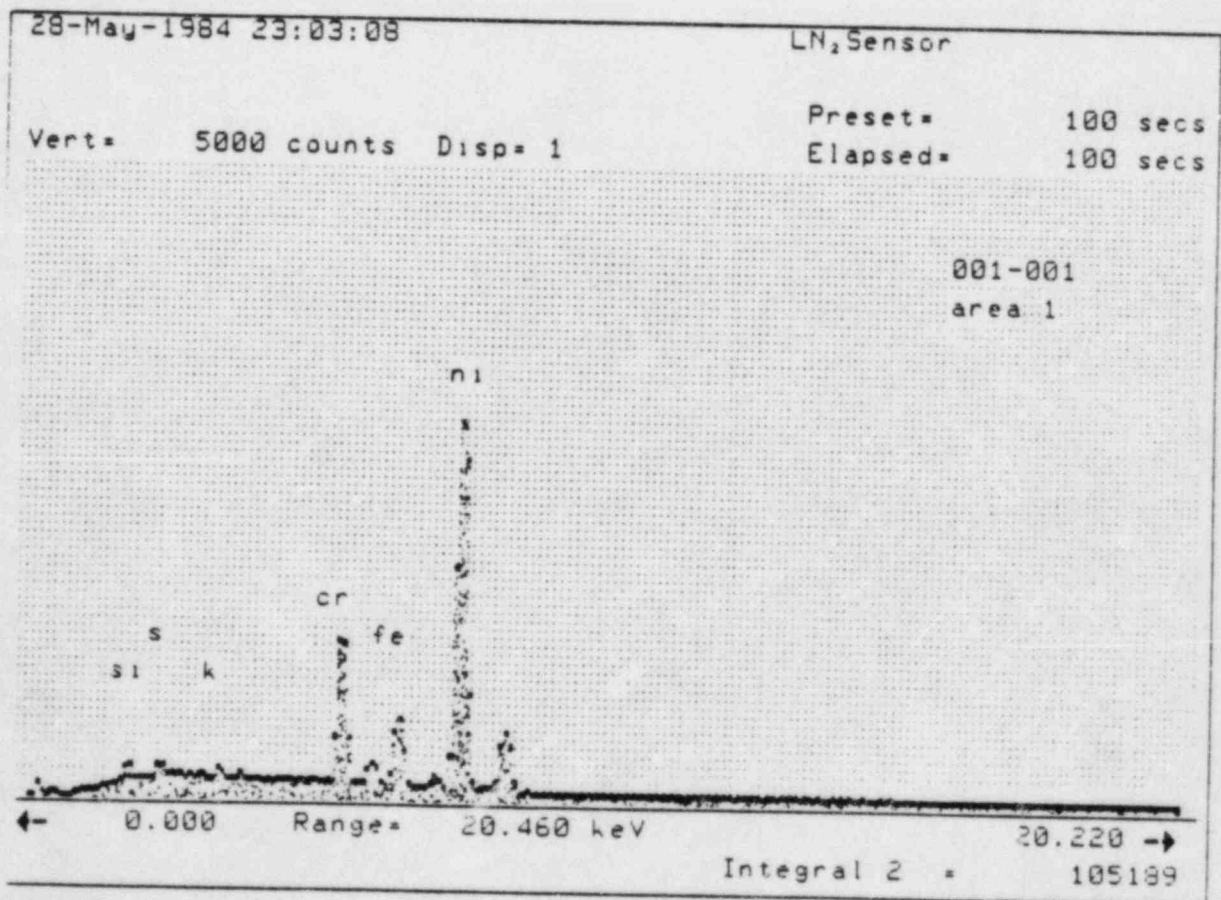Results from the Area Shown (continued).

Figure 22. Scanning Electron Micrograph of a Crack Tip and EDS Analysis Results from the Area Shown. (Neg. #67767, 250X)
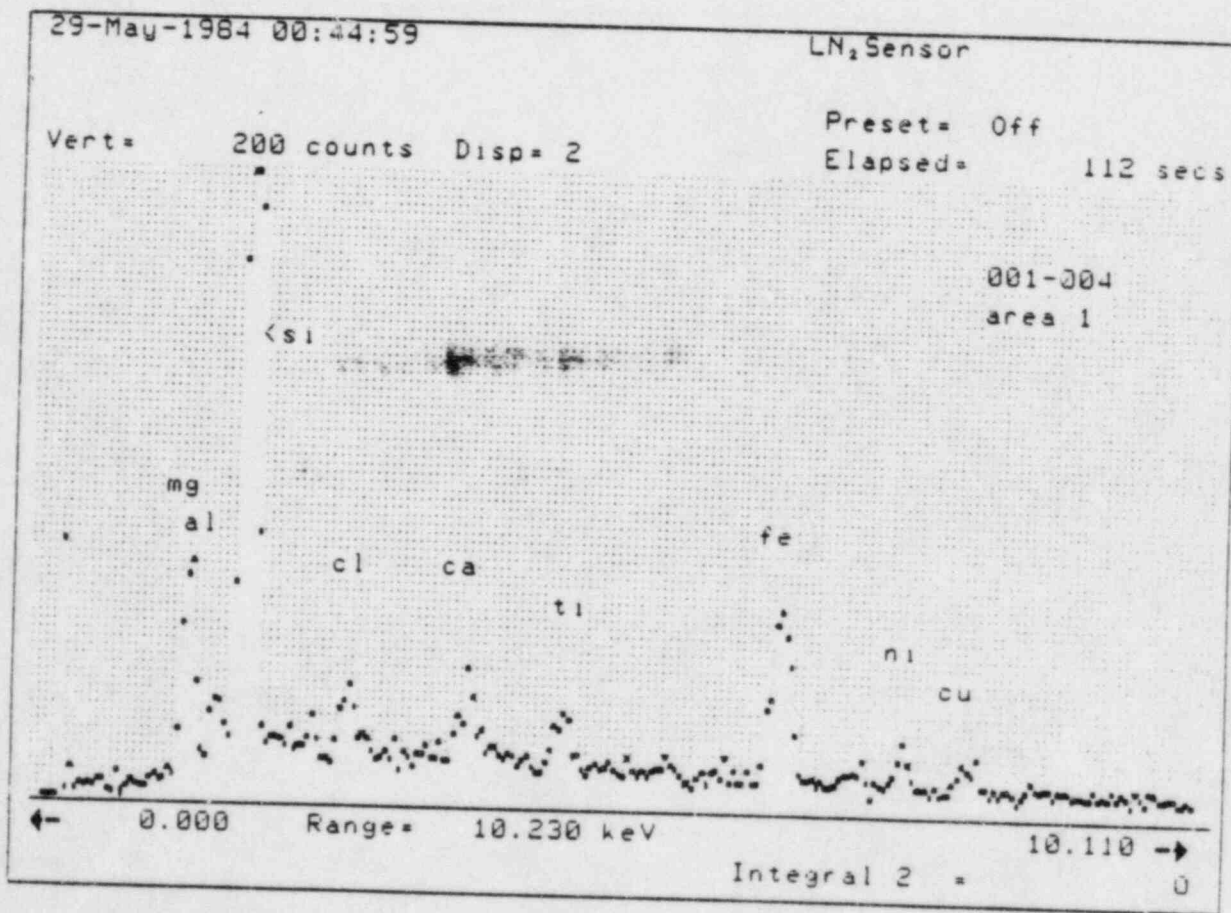
Figure 23. Scanning Electron Micrograph of a Crack Area and EDS Analysis Results of a Si Rich Particle. (Neg. #67770, 1000X)